



1 **SM2RAIN-ASCAT (2007-2018): global daily satellite rainfall**  
2 **from ASCAT soil moisture**

3

4 Luca Brocca<sup>1\*</sup>, Paolo Filippucci<sup>1</sup>, Sebastian Hahn<sup>2</sup>, Luca Ciabatta<sup>1</sup>, Christian Massari<sup>1</sup>,  
5 Stefania Camici<sup>1</sup>, Lothar Schüller<sup>3</sup>, Bojan Bojkov<sup>3</sup>, Wolfgang Wagner<sup>2</sup>

6

7

8 [1]{Research Institute for Geo-Hydrological Protection, National Research Council, Perugia, Italy }

9 [2]{Department of Geodesy and Geoinformation, Vienna University of Technology, Vienna, Austria }

10 [3]{European Organisation for the Exploitation of Meteorological Satellites, Darmstadt, Germany }

11

12

13

14

15

16

17

18

19

20

21

\* Correspondence to: Ph.D. Luca Brocca, Research Institute for Geo-Hydrological Protection, National Research Council, Via della Madonna Alta 126, 06128 Perugia, Italy. Tel: +39 0755014418 Fax: +39 0755014420 E-mail: [luca.brocca@irpi.cnr.it](mailto:luca.brocca@irpi.cnr.it).



## 22 **Abstract**

23 Long-term gridded precipitation products are crucial for several applications in  
24 hydrology, agriculture and climate sciences. Currently available precipitation products obtained  
25 from rain gauges, remote sensing and meteorological modelling suffer from space and time  
26 inconsistency due to non-uniform density of ground networks and the difficulties in merging  
27 multiple satellite sensors. The recent “bottom up” approach that uses satellite soil moisture  
28 observations for estimating rainfall through the SM2RAIN algorithm is suited to build long-  
29 term and consistent rainfall data record as a single polar orbiting satellite sensor is used.

30 We exploit here the Advanced SCATterometer (ASCAT) on board three Metop satellites,  
31 launched in 2006, 2012 and 2018. The continuity of the scatterometer sensor on European  
32 operational weather satellites is ensured until mid-2040s through the Metop Second Generation  
33 Programme. By applying SM2RAIN algorithm to ASCAT soil moisture observations a long-  
34 term rainfall data record can be obtained, also operationally available in near real time. The  
35 paper describes the recent improvements in data pre-processing, SM2RAIN algorithm  
36 formulation, and data post-processing for obtaining the SM2RAIN-ASCAT global daily rainfall  
37 dataset at 12.5 km sampling (2007-2018). The quality of SM2RAIN-ASCAT dataset is assessed  
38 on a regional scale through the comparison with high-quality ground networks in Europe,  
39 United States, India and Australia. Moreover, an assessment on a global scale is provided by  
40 using the Triple Collocation technique allowing us also the comparison with other global  
41 products such as the latest European Centre for Medium-Range Weather Forecasts reanalysis  
42 (ERA5), the Global Precipitation Measurement (GPM) mission, and the gauge-based Global  
43 Precipitation Climatology Centre (GPCC) product.

44 Results show that the SM2RAIN-ASCAT rainfall dataset performs relatively well both  
45 at regional and global scale, mainly in terms of root mean square error when compared to other  
46 datasets. Specifically, SM2RAIN-ASCAT dataset provides better performance better than  
47 GPM and GPCC in the data scarce regions of the world, such as Africa and South America. In  
48 these areas we expect the larger benefits in using SM2RAIN-ASCAT for hydrological and  
49 agricultural applications.

50 The SM2RAIN-ASCAT dataset is freely available at  
51 <https://doi.org/10.5281/zenodo.2591215>.

52 *Keywords:* Rainfall, Soil moisture, ASCAT, SM2RAIN, Remote Sensing.



## 53 1 Introduction

54         Rainfall is ranked the first among the Essential Climate Variable by the Global Climate  
55         Observing System (GCOS) as it represents the most important variable in many applications in  
56         geosciences ([Maggioni and Massari, 2018](#)). Near real-time rainfall data are needed for the  
57         mitigation of the impacts of natural disasters such as floods and landslides (e.g., [Wang et al.,](#)  
58         [2107](#); [Camici et al., 2018](#); [Brunetti et al., 2018](#); [Kirschbaum and Stanley, 2018](#)) while long-  
59         term rainfall record are essential for drought monitoring (e.g., [Forootan et al., 2019](#)), water  
60         resources management (e.g., [Abera et al., 2017](#)) and climate studies (e.g., [Herold et al., 2016](#);  
61         [Pendergrass and Knutti, 2018](#)). Additional applications in which rainfall plays a crucial role are  
62         weather forecasting, agricultural planning, vector-borne and waterborne diseases (e.g., [Rinaldo](#)  
63         [et al., 2012](#); [Thaler et al., 2018](#)).

64         Three different techniques can be used for estimating rainfall: ground measurements,  
65         meteorological modelling and remote sensing. Ground measurements are based on rain gauges  
66         and meteorological radars ([Lanza et al., 2009](#)), but also new approaches such as microwave  
67         links are being developed (e.g., [Overeem et al., 2011](#)). These measurements guarantee high  
68         accuracy but suffer in many regions from limited spatial coverage ([Kidd et al., 2017](#)).  
69         Alternatively, meteorological models (e.g., reanalysis) are used to estimate rainfall mainly in  
70         areas without ground reliable observations ([Ebert et al., 2007](#)). The uncertainties associated  
71         with these estimates can be large, mainly in areas where ground observations are scarce  
72         ([Massari et al., 2017a](#)). Therefore, to fill the gaps in the spatial coverage of ground  
73         measurements, and to improve the estimates obtained by models, different remote sensing  
74         techniques have been developed in the last 30 years ([Hou et al., 2014](#)). The standard methods  
75         for measuring rainfall from space are based on instantaneous measurements obtained from  
76         microwave radiometers, radars, and infrared sensors ([Kidd and Levizzani, 2011](#)). These  
77         methods are based on the inversion of the atmospheric signals reflected or radiated by  
78         atmospheric hydrometeors, i.e., a “top down” approach ([Brocca et al., 2014](#)).

79         The most recent and successful example of satellite precipitation estimates is represented  
80         by the Integrated Multi-Satellite Retrievals for GPM (IMERG) of the Global Precipitation  
81         Measurement (GPM) mission ([Hou et al., 2014](#)) which provide high spatial (0.1°) and temporal  
82         (30-minute) resolution and quasi-global coverage (+/-60°). To obtain such resolution and  
83         coverage, the IMERG products use a constellation of polar and geostationary satellite sensors  
84         operating in the microwave and infrared bands. However, the use of multiple sensors has some



85 problems, including: the inconsistency between rainfall estimates from different sensors  
86 (intercalibration problem), the difficulties in collecting observations from multiple space  
87 agencies (i.e., problem of delivering the products in near real-time), and the high costs for the  
88 operation and the maintenance of the overall constellation. Moreover, as the top down approach  
89 requires the merging of instantaneous rainfall measurements from multiple sensors, the failure  
90 of one of them may imply a significant degradation in the accuracy of accumulated rainfall  
91 estimate due to the high temporal variability of rainfall ([Trenberth and Asrar, 2014](#)).

92 In recent years, a new “bottom up” approach has emerged that uses satellite soil moisture  
93 observations to infer, or to correct, rainfall over land ([Brocca et al., 2013a](#); [Crow et al., 2009](#);  
94 [Pellarin et al., 2013](#); [Wanders et al., 2015](#)). The major difference between the bottom up and  
95 top down approaches is in the type of measurement; i.e., accumulated rainfall with the bottom  
96 up method and instantaneous rainfall rates with the top down method. This difference makes  
97 the two approaches highly complementary and their integration has been already successfully  
98 tested and demonstrated in several recent studies (e.g., [Brocca et al., 2016](#); [Ciabatta et al., 2017](#);  
99 [Chiaravallotti et al., 2018](#); [Massari et al. 2019](#)). When accumulated rainfall estimates are needed  
100 (e.g., daily rainfall), the bottom up approach has the advantage to require a much lower number  
101 of measurements and, hence, of satellite sensors. The limitations of the bottom up approach are  
102 the possibility to estimate only terrestrial rainfall and its dependence on land characteristics  
103 (e.g., low accuracy for dense vegetation coverage and complex topography, [Brocca et al., 2014](#)).

104 The bottom up approach has been applied over a range of scales: global ([Crow et al.,](#)  
105 [2011](#); [Brocca et al., 2014](#); [Ciabatta et al., 2018](#)), continental ([Wanders et al., 2015](#); [Brocca et](#)  
106 [al., 2016](#)), and local ([Massari et al., 2014](#); [Brocca et al., 2015](#); [Román-Cascón et al., 2017](#)) scale.  
107 Moreover, different satellite soil moisture products have been considered including SMOS (Soil  
108 Moisture Ocean Salinity mission, [Brocca et al., 2016](#)), ASCAT (Advanced SCATterometer,  
109 [Brocca et al., 2017](#)), AMSR-E (Advanced Microwave Scanning Radiometer, [Crow et al., 2009](#)),  
110 and SMAP (Soil Moisture Active and Passive, [Koster et al., 2016](#); [Tarpanelli et al., 2017](#); [Zhang](#)  
111 [et al., 2019](#)). First studies employing satellite rainfall estimates obtained through the bottom up  
112 approach for hydrological and water resources applications have been recently published (e.g.,  
113 [Ciabatta et al., 2016](#); [Abera et al., 2017](#); [Brunetti et al., 2018](#); [Camici et al., 2018](#)). These studies  
114 have highlighted the large potential of this technique as a complimentary and useful approach  
115 for estimating rainfall from space, and have also shown its main limitations. Specifically, the



116 temporal resolution and the accuracy of satellite soil moisture products play a fundamental role  
117 in determining the accuracy of the bottom up rainfall estimates.

118 In this study, we describe the newly developed SM2RAIN-ASCAT rainfall dataset  
119 covering the period 2007-2018 and characterized by a spatial/temporal sampling of 12.5 km/1-  
120 day. The new SM2RAIN-ASCAT dataset is obtained from the application of SM2RAIN  
121 algorithm ([Brocca et al., 2014](#)) to ASCAT soil moisture data, and it is the first SM2RAIN-  
122 ASCAT dataset available at the same spatial resolution as the ASCAT soil moisture dataset  
123 (previous datasets have been under-sampled at 0.5- and 1-degree resolution). Moreover, we  
124 have included the latest improvements in pre- and post-processing of soil moisture and rainfall  
125 data as well as in the SM2RAIN algorithm. The main differences with the SM2RAIN-CCI  
126 rainfall dataset ([Ciabatta et al., 2018](#)) are the input soil moisture dataset (the input of  
127 SM2RAIN-CCI is the European Space Agency Climate Change Initiative Soil Moisture, ESA  
128 CCI soil moisture, product, [Dorigo et al., 2017](#)), and the time coverage (SM2RAIN-CCI spans  
129 the period 1998-2015). Technically, the use of the same satellite sensor in SM2RAIN-ASCAT  
130 dataset is preferable to ensure consistency between soil moisture estimates over time to which  
131 the SM2RAIN algorithm is highly sensitive.

132 The purpose of this study is twofold. As a first objective, we have applied SM2RAIN  
133 algorithm at 1009 points uniformly distributed in the United States, Italy, India and Australia  
134 for testing different configurations of data pre-/post-processing and SM2RAIN model equation.  
135 This analysis has allowed us to select the best configuration that is implemented on a global  
136 scale for obtaining the SM2RAIN-ASCAT dataset. The second objective is the assessment of  
137 the global scale SM2RAIN-ASCAT dataset through the comparison with reference datasets and  
138 by exploiting the Triple Collocation (TC) approach ([Massari et al., 2017a](#)). As reference  
139 datasets we have used high-quality local raingauge networks from 2013 to 2017 in the United  
140 States, Italy, India and Australia and three additional global datasets: the latest reanalysis of the  
141 European Centre for Medium-Range Weather Forecasts (ECMWF), ERA5, the gauge-based  
142 Global Precipitation Climatology Centre (GPCC), and the GPM IMERG product (Early Run  
143 version).

## 144 2 Datasets

145 Nine different datasets have been collected for this study which are based on remote  
146 sensing, ground observations and reanalysis. Refer to **Table 1** for a summary of the datasets.



147           The main input dataset for producing SM2RAIN-ASCAT dataset is the ASCAT soil  
148 moisture data record provided by the “EUMETSAT Satellite Application Facility on Support  
149 to Operational Hydrology and Water Management (H SAF)”. ASCAT, currently on board  
150 Metop-A (launched on October 2006), Metop-B (September 2012) and Metop-C (November  
151 2018) satellites, is a scatterometer operating at C-band (5.255 GHz) and, by using the TU Wien  
152 algorithm ([Wagner et al., 2013](#)) the H SAF provides a soil moisture product characterized by  
153 12.5 km spatial sampling. The temporal sampling is varying as a function of latitude and the  
154 number of satellites: by using Metop-A only a daily sampling is obtained, by using Metop-A  
155 and Metop-B two observations per day are available at mid-latitudes. Here we have used the  
156 H SAF ASCAT soil moisture data record (using Metop-A and Metop-B) available through the  
157 product H113 ([PUM, 2018](#)) from 2007 to 2017 and its extension product H114 for the year  
158 2018.

159           Three datasets obtained from the latest reanalysis of ECMWF, i.e., ERA5, have been  
160 used. ERA5 reanalysis is characterized by a spatial resolution of ~36 km and hourly temporal  
161 resolution. ERA5 is available from the Copernicus Climate Change service and the datasets  
162 cover the period 1979 to present. We have extracted hourly observations for the period 2007-  
163 2018 for three variables: evaporation, soil temperature for the first layer (0-7 cm) and total  
164 rainfall (computed as the difference between total precipitation and snowfall). Evaporation data  
165 are used as additional input to the SM2RAIN algorithm and soil temperature data for masking  
166 periods with frozen soils. Total rainfall has been considered as a benchmark for the calibration  
167 of global SM2RAIN parameter values (see next section).

168           Ground-based rainfall datasets from regional networks have been also collected including  
169 the Climate Prediction Center (CPC) Unified Gauge-Based Analysis of Daily Precipitation in  
170 the United States, the gridded rainfall data provided by ~3000 stations of the National  
171 Department of Civil Protection in Italy ([Ciabatta et al., 2017](#)), the India Meteorological  
172 Department (IMD, [http://www.imd.gov.in/pages/services\\_hydromet.php](http://www.imd.gov.in/pages/services_hydromet.php)) rainfall observations  
173 in India, and the Australia Water Availability Project (AWAP, <http://www.bom.gov.au/jsp/awap/rain/index.jsp>) gridded rainfall data in Australia. These  
174 datasets have been used firstly for the selection of the optimal configuration of SM2RAIN  
175 implementation. For that, 1009 points uniformly distributed over the four regions have been  
176 selected. Secondly, the regional networks have been used for the assessment of the global  
177 SM2RAIN-ASCAT rainfall product at regional scale.  
178



179           The ERA5 and local rainfall datasets have been regrided over the ASCAT grid (12.5 km)  
180 through the nearest neighbouring method and resampled at daily time scale as accumulated  
181 rainfall from 00:00 to 23:59 UTC. The ERA5 evaporation and soil temperature data are also  
182 regrided to the same grid and aggregated at daily scale as accumulated and average value from  
183 00:00 to 23:59 UTC, respectively.

184           For the global assessment of SM2RAIN-ASCAT, two additional rainfall datasets have  
185 been considered: Global Precipitation Climatology Centre (GPCC) Full Data Daily Product  
186 ([Schamm et al., 2015](#)) and GPM IMERG Early Run product ([Hou et al., 2014](#)), hereinafter  
187 referred to as GPM-ER. Due to the availability of GPM-ER from April 2014, the global analysis  
188 has been carried out in the 4-year period from January 2014 to December 2018. Moreover, for  
189 the global inter-comparison all the datasets (SM2RAIN-ASCAT, ERA5, GPCC, and IMERG-  
190 ER) have been regrided at 0.25-degree resolution by spatial averaging the pixels contained in  
191 each 0.25-degree cell for SM2RAIN-ASCAT and GPM-ER, and by selecting the nearest pixel  
192 for ERA5 and GPCC.

### 193   **3 Methods**

194           In the following, the methodology used for obtaining the SM2RAIN-ASCAT dataset is  
195 described. Specifically, three steps are carried out (see [Figure 1](#)): 1) surface soil moisture data  
196 pre-processing, 2) SM2RAIN algorithm, and 3) rainfall data post-processing.

#### 197   **3.1 Soil moisture data pre-processing**

198           The ASCAT surface soil moisture product is provided as relative soil moisture (between  
199 0 and 1) at the overpass time of the satellite sensor. For the application of SM2RAIN algorithm,  
200 data should be equally spaced in time and hence, we have linearly interpolated in time soil  
201 moisture observations every 24 hours, 12 hours and 8 hours. In a preliminary test (not shown  
202 for brevity), we have tested the three sampling frequencies with the baseline formulation for  
203 SM2RAIN ([equation 6](#), see below). The best performances have been obtained with 12 hours  
204 sampling, particularly from 2013 to 2018 in which both Metop-A and -B are available.  
205 Therefore, 12 hours sampling has been used in the following analyses.

206           One of the major problems in using satellite soil moisture observations for rainfall  
207 estimation is related to the high frequency fluctuations caused by measurement and retrieval  
208 errors. If positive, such fluctuations are interpreted erroneously as rainfall by SM2RAIN



209 algorithm. Therefore, satellite surface soil moisture data need to be filtered before being used  
210 as input into SM2RAIN. In previous studies, the exponential filtering has been considered  
211 ([Wagner et al., 1999](#)). The exponential filter, also known as Soil Water Index (SWI), has been  
212 used for filtering surface soil moisture time series as a function of a single parameter,  $T$ , i.e.,  
213 the characteristic time length. In this study, we have tested two additional filtering methods.  
214 The first one is an extension of the exponential filter in which the  $T$  parameter is assumed to be  
215 varying with soil moisture as proposed in [Brocca et al. \(2013b\)](#). Specifically,  $T$  decreases with  
216 increasing soil moisture through a 2-parameter power law. Therefore, the data are filtered more  
217 during dry conditions. The third approach that we have implemented is a discrete wavelet filter  
218 (similar to [Massari et al., 2017b](#)). The discrete wavelet filter cuts the higher frequencies of the  
219 signal, typically characterized by noises, over a threshold selected through the principle of  
220 Stein's Unbiased Risk at multiple levels. We have found the Daubechies wavelets to be the most  
221 appropriate functions because their shape and the shape of the soil moisture signal is similar.  
222 Therefore, we have implemented a Daubechies-based wavelet filter in which the filtering level  
223 is optimized.

224 For all the filtering approaches, the parameter values of the filters have been optimized  
225 point-by-point in order to reproduce the reference rainfall observations.

### 226 3.2 SM2RAIN algorithm and calibration

227 The SM2RAIN algorithm is based on the inversion of the soil water balance equation and  
228 allows to estimate the amount of water entering the soil by using as input soil moisture  
229 observations from in situ or satellite sensors (e.g., [Brocca et al., 2013a; 2014; 2015](#); [Koster et al., 2016](#);  
230 [Ciabatta et al., 2017](#); [Massari et al., 2014](#)). Specifically, the soil water balance  
231 equation can be described by the following equation (over non-irrigated areas):

$$232 \quad nZ \frac{dS(t)}{dt} = p(t) - g(t) - sr(t) - e(t) \quad (1)$$

233 where  $n$  [-] is the soil porosity,  $Z$  [mm] is the soil layer depth,  $S(t)$  [-] is the relative  
234 saturation of the soil or relative soil moisture,  $t$  [days] is the time,  $p(t)$  [mm/day] is the rainfall  
235 rate,  $g(t)$  [mm/day] is the drainage (deep percolation plus subsurface runoff) rate,  $sr(t)$   
236 [mm/day] is the surface runoff rate and  $e(t)$  [mm/day] is the actual evapotranspiration rate.

237 For estimating the rainfall rate, *equation (1)* is applied only during rainfall periods and,  
238 hence, some of the components of the equation can be considered as negligible. For instance,





239 the actual evapotranspiration rate during rainfall is quite low due to the presence of clouds and,  
 240 hence, the absence of solar radiation. Similarly, the surface runoff rate, i.e., the water that does  
 241 not infiltrate into the soil and flows at the surface to the watercourses, is much lower than the  
 242 rainfall rate, mainly if *equation (1)* is applied at coarse spatial resolution (20 km), i.e., with  
 243 satellite soil moisture data. Indeed, most of water becomes runoff flowing in the subsurface,  
 244 and also the part that does not infiltrate, due to almost impervious land cover or soil, may re-  
 245 infiltrate downstream within a pixel at 20 km scale.

246 Following the indications obtained in [Brocca et al. \(2015\)](#), we have assumed the surface  
 247 runoff rate,  $sr(t)$ , as negligible (i.e., Dunnian runoff) and we have rearranged *equation (1)* for  
 248 estimating the rainfall rate:

$$249 \quad p(t) = nZ \frac{dS(t)}{dt} - g(t) - e(t) \quad (2)$$

250 In this study, we have considered different formulations for equation (2) by varying the  
 251 drainage rate as:

$$252 \quad g(t) = K_s S(t)^m \quad (3.1)$$

$$253 \quad g(t) = K_s S(t)^{\lambda+1} \left[ 1 - \left( 1 - S(t)^{\frac{\lambda+1}{\lambda}} \right)^{\frac{\lambda}{\lambda+1}} \right]^2 \quad (3.2)$$

$$254 \quad g(t) = K_s S(t)^\tau \left[ 1 - \left( 1 - S(t)^{\frac{1}{m}} \right)^m \right]^2 \quad (3.3)$$

255 where  $K_s$  [mm/day] is the saturated hydraulic conductivity,  $m$  [-] and  $\lambda$  [-] are exponents related  
 256 to the pore size distribution index, and  $\tau$  is the tortuosity index. Specifically, the three equations  
 257 represent the hydraulic conductivity - soil moisture formulation by Brooks-Corey (3.1), van  
 258 Genuchten (3.2), and Mualem-van Genuchten (3.3).

259 The actual evapotranspiration rate has been considered as an additional input, together  
 260 with soil moisture, here obtained from ECMWF reanalysis ERA5:

$$261 \quad e(t) = K_c ET_{ERA5}(t) \quad (4)$$

262 where  $ET_{ERA5}(t)$  [mm/day] is the actual evapotranspiration rate obtained from ERA5 reanalysis  
 263 and  $K_c$  [-] is a correction factor for taking into account potential bias in ERA5 estimates.



264 Moreover, we have considered an additional formulation in which  $Z$  is a function of soil  
265 moisture taking into account the different penetration depth of satellite sensors as a function of  
266 wetness conditions:

$$267 \quad Z = Z[0.1 + (1 - S(t)^c)] \quad (5)$$

268 where  $c$  exponent determines the rate of decrease of penetration depth with increasing soil  
269 moisture.

270 Accordingly, we have used different formulations for equation (2) that are compared with  
271 the baseline equation used in previous studies (e.g., [Brocca et al., 2014](#)):

$$272 \quad p(t) = Zn \frac{dS(t)}{dt} + K_s S(t)^m \quad (6)$$

273 In synthesis, we have investigated 3 different configurations (total of 5 options) for: 1)  
274 selecting the best equation for the drainage rate (*equations 3*), 2) testing the possibility to  
275 include the evapotranspiration component (*equation 4*), and 3) testing the use of a variable  
276 penetration depth with soil moisture conditions (*equation 5*). Each new configuration has been  
277 compared with the baseline (*equation 6*) in order to select the best configuration for SM2RAIN  
278 algorithm (see *Figure 1*). For all configurations, negative rainfall values, that might occur  
279 during some dry-down cycles, have been set equal to zero.

### 280 **3.3 Rainfall data post-processing**

281 The use of satellite soil moisture observations for obtaining rainfall estimates is affected  
282 by errors in the input data and in the retrieval algorithm SM2RAIN. The correction of the  
283 overall bias in the climatology is a simple and effective approach for mitigating part of such  
284 errors. Specifically, we refer here to a static correction procedure that once calibrated for a time  
285 period can be applied in the future periods, also for real-time products. We have implemented  
286 two different approaches for climatological correction: 1) a cumulative density function (CDF)  
287 matching approach at daily time scale, and 2) a monthly correction approach. Specifically, the  
288 implemented CDF matching approach is a 5-order polynomial correction as described in [Brocca  
289 et al. \(2011\)](#) for matching the CDF of estimated rainfall with respect to reference rainfall, in  
290 which the CDF are computed over the whole calibration period at daily time scale. The monthly  
291 correction approach computes the monthly ratios between the climatology of estimated and  
292 reference rainfall, i.e., 12 correction factors per pixel. Then, the SM2RAIN-estimated rainfall



293 is multiplied for the monthly correction factors to obtain the climatologically corrected  
294 SM2RAIN-estimated rainfall.

### 295 **3.4 Triple collocation analysis**

296 For the global assessment of satellite, reanalysis and gauge-based rainfall products we  
297 have used the Triple Collocation (TC) technique. TC can theoretically provide error and  
298 correlations of three products (a triplet) given that each of the three products is afflicted by  
299 mutually independent errors. Therefore, in principle, TC can be used for assessing the quality  
300 of satellite products without using ground observations ([Massari et al., 2017a](#)). In this study,  
301 we have implemented the same procedure as described in [Massari et al. \(2017\)](#) and we refer the  
302 reader to this study for the analytical details. In synthesis, by using the extended TC method  
303 firstly proposed by [McColl et al. \(2014\)](#), it is possible to estimate the temporal correlation,  $R_{TC}$ ,  
304 of each rainfall product in the triplets with the truth.

### 305 **3.5 Performance scores**

306 Several metrics have been used to assess the product performance during the validation  
307 period. As continuous scores we have computed the Pearson's correlation coefficient (R), the  
308 root mean square error (RMSE), the mean error between estimated and reference rainfall  
309 (BIAS), and the ratio of temporal variability of estimated and reference rainfall (STDRATIO).  
310 Continuous scores have been computed on a pixel-by-pixel basis by considering 1 day of  
311 accumulated rainfall. Moreover, three categorical scores, i.e. Probability of Detection (POD),  
312 False Alarm Ratio (FAR) and Threat Score (TS), have been computed. POD is the fraction of  
313 correctly identified rainfall events (optimal value  $POD=1$ ), FAR is the fraction of predicted  
314 events that are non-events (optimal value  $FAR=1$ ), while TS provides a combination of the  
315 other two scores (optimal value  $TS=1$ ). The categorical assessment is carried out by considering  
316 a rainfall threshold of 0.5 mm/day (instead of 0 mm/day) in order to exclude spurious events  
317 that might be due to rainfall interpolation/regridding in the reference datasets. For a complete  
318 description of the categorical scores the reader is referred to [Brocca et al. \(2014\)](#).

## 319 **4 Results**

320 The results are split in three parts: 1) selection of the optimal configuration of SM2RAIN  
321 through the assessment at 1009 points, 2) generation of global SM2RAIN-ASCAT rainfall



322 dataset, and 3) regional assessment of SM2RAIN-ASCAT with gauge-based rainfall datasets  
323 and global assessment through TC.

#### 324 **4.1 Selection of the best SM2RAIN processing configuration at 1009 points**

325 As a first step we have co-located satellite soil moisture data from ASCAT, ground-based  
326 rainfall observations and actual evapotranspiration data from ERA5 in space and time at 1009  
327 points. We have selected 1009 points uniformly distributed, instead of the whole region, in  
328 order to test multiple configuration at reasonable computational cost. These datasets are made  
329 freely available here (<https://doi.org/10.5281/zenodo.2580285>, Brocca, 2019) for those  
330 interested to test alternative approaches for rainfall estimation from ASCAT soil moisture.  
331 Specifically, we have considered the period 2013-2016, 2013-2014 for the calibration and  
332 2015-2016 for the validation; in the sequel only the results in the validation period are shown.  
333 The reference configuration, REF, as used in previous SM2RAIN applications (e.g., Brocca et  
334 al., 2014), uses the SWI for data filtering, the SM2RAIN formulation as in *equation (6)*, and  
335 no climatological correction. Results in the validation period are shown in *Figure 2A* in terms  
336 of temporal R against reference data. As shown, the median R for all points is equal to 0.60,  
337 with better results in Italy (median R=0.67, see boxplots) and similar results in the other 3  
338 regions (median R=0.60 and 0.59). These results are in line with previous studies (e.g., Ciabatta  
339 et al., 2017; Tarpanelli et al., 2017) carried out in Italy and India and highlight the potential of  
340 ASCAT soil moisture observations to provide daily rainfall estimates. *Figure 3* (first column)  
341 shows the results for the different performance metrics; in the last column the results obtained  
342 with GPM-ER are shown for comparison. Very good statistics have been obtained in terms of  
343 RMSE and BIAS but a tendency to underestimate the observed rainfall variability (median  
344 STDRATIO=0.60) and medium-high probability of false alarm (median FAR=0.53). The other  
345 scores are similar, or slightly lower than those obtained through GPM-ER.

346 The first test has been dedicated to the filtering of soil moisture data by using three  
347 approaches: 1) SWI, i.e., the REF configuration, 2) SWI with T varying with soil moisture,  
348 SWI-Tvar, and 3) the discrete wavelet filtering, WAV. *Figure 3* shows in the first three columns  
349 the summary of the performance scores highlighting that the SWI-Tvar configuration is  
350 performing the best, even though the differences with REF configuration are small. *Figure 2b*  
351 shows the R map for SWI-Tvar configuration while in *Figure 2c* the differences in R-values  
352 with REF are displayed. Improved performance in terms of R is visible over most of the pixels  
353 except in central Australia.



354 The second test has been performed on the SM2RAIN equation by using different  
355 drainage functions (VGEN and MUA configurations), by adding the evapotranspiration  
356 component (EVAP), and by considering the variability of sensing depth,  $Z$ , with soil moisture  
357 (ZVAR); the details of the different configurations are given in **Table 2**. VGEN, MUA and  
358 ZVAR configurations are characterized by lower performances than REF (see **Figure 3**,  
359 columns 4, 5 and 7), even though MUA and ZVAR incorporate an additional parameter to be  
360 calibrated (and, hence, better performance was expected). The addition of evapotranspiration  
361 brings a slight improvement with respect to REF (see **Figure 3**, columns 6), with results similar  
362 to SWI-Tvar. Larger improvements are obtained over areas in which evapotranspiration is more  
363 important, e.g., in the south-western United States and central western Australia. In India and  
364 Italy, the results are very similar to REF. However, EVAP configuration requires actual  
365 evapotranspiration data from ERA5 as additional input and such data might be not available for  
366 the implementation of the processing algorithm in an operational context.

367 The final test has been done by applying the daily CDF matching, BC-CDF, and monthly  
368 correction factors, BC-MON, for correcting the climatological bias in SM2RAIN-derived  
369 rainfall estimates; results are shown in columns 8 and 9 of **Figure 3**. For these two  
370 configurations, the improvements with respect to REF are evident but with different magnitude  
371 for the different scores. BC-CDF improves significantly STDRATIO, TS and FAR with a slight  
372 deterioration in R and RMSE. BC-MON shows the highest R-values among all configurations  
373 with the larger improvements in India, Italy and United States. However, the improvement in  
374 terms of STDRATIO, TS and FAR is less important than BC-CDF. Therefore, depending on  
375 which score is assumed more important, one of the two configurations can be selected. If  
376 compared with GPM-ER, BC-CDF and BC-MON configurations show similar results with  
377 larger positive differences, in terms of RMSE, BIAS, STDRATIO and POD; R values are  
378 slightly better for GPM-ER that is also much better in terms of TS and FAR.

379 **Figure 4** shows time series of rainfall averaged over the four regions as obtained from  
380 ground observations and from BC-MON configuration. The agreement of spatially averaged  
381 rainfall with observations is high with R-values greater than 0.83, very low BIAS and  
382  $KGE > 0.67$ . Moreover, regional scale rainfall events are correctly reproduced both in terms of  
383 timing and magnitude.



#### 384 4.2 Generation of SM2RAIN-ASCAT dataset

385 Based on the tests performed in the previous paragraph, we have selected the best  
386 configuration using SWI-Tvar for filtering, Brooks-Corey function for losses, and the monthly  
387 correction approach for climatological correction. The addition of evapotranspiration  
388 component, even though showing some improvements, has been not used in view of an  
389 operational implementation of the method. The monthly correction approach has been selected  
390 as R and RMSE scores have been considered more important.

391 The selected configuration has been applied on a global scale to 839826 points over which  
392 ASCAT soil moisture observations are available. As reference dataset for calibrating the  
393 filtering, SM2RAIN, and post-processing parameter values, the ERA5 rainfall has been used  
394 mainly because of its higher spatial resolution compared to GPCC (36 km versus 100 km).  
395 However, we have also tested the use of the two datasets for calibration at randomly chosen  
396 20000 points which showed that the estimated rainfall in the two calibration tests is very similar.  
397 For instance, the median R between the two SM2RAIN-ASCAT dataset is higher than 0.90 (not  
398 shown for brevity). This result clearly demonstrate that the selection of reference dataset has a  
399 small influence on SM2RAIN-derived rainfall that is mostly driven from soil moisture temporal  
400 fluctuations. Additionally, considering the improved ASCAT coverage after 2013, the  
401 calibration has been split from 2007 to 2012 (Metop-A) and from 2013 to 2018 (Metop-A and  
402 -B). Finally, being aware of the regions in which ASCAT soil moisture product is performing  
403 not good, we have flagged rainfall observations in space and time when the data are supposed  
404 to be less reliable. In space, we have used the committed area mask developed for ASCAT soil  
405 moisture product ([PVR 2017](#)) in which the quality of ASCAT soil moisture is found to be good,  
406 a frozen probability mask and a topographic complexity mask. In time, we have considered the  
407 soil temperature data from ERA5 and flagged the observations with soil temperature values  
408 between 0°C and 3°C as temporary frozen soil and below 3°C as frozen soil. As many  
409 applications require continuous data, we have preferred to flag the data instead of removing  
410 them with an expected loss of accuracy.

411 The SM2RAIN-ASCAT dataset so obtained has a spatial sampling of 12.5 km, a daily  
412 temporal resolution and covers the 12-year period 2007-2018. **Figure 5** shows R and RMSE  
413 values between SM2RAIN-ASCAT and ERA5 in a single map. Green light colours indicate  
414 very good performance with high R and low RMSE, orange to red colours indicate low R and  
415 high RMSE, while black indicates low RMSE and R highlighting areas in which rainfall



416 occurrence and variability is very low (e.g., Sahara Desert, high latitudes). The dataset has been  
417 found to perform accurately (high R and low RMSE) in western United States, Brazil, southern  
418 and western South America, southern Africa, Sahel, southern-central Eurasia, and Australia.  
419 The areas in which SM2RAIN-ASCAT is characterized by lower accuracy are those with dense  
420 vegetation (Amazon, Congo, and Indonesia), with complex topography (e.g., Alps, Himalaya,  
421 Andes), at high latitudes and Saharan and Arabian deserts. In these areas it is well-known that  
422 ASCAT soil moisture product has limitations (e.g., [Wagner et al., 2013](#)), and generally the  
423 retrieval of soil moisture from remote sensing is more challenging. The median R and RMSE  
424 values are equal to 0.56 and 3.06 mm/day, with slightly better scores in the period 2013-2018  
425 (R=0.57, RMSE=2.95), thanks to the availability of ASCAT on both Metop-A and -B.

#### 426 **4.3 Regional and global assessment of SM2RAIN-ASCAT dataset**

427 By using all the pixels included in the four regions (Italy, United States, India and  
428 Australia), for a total of 29843 points, the new SM2RAIN-ASCAT rainfall dataset has been  
429 compared with reference rainfall observations in *Figure 6*, by considering the whole period  
430 2007-2018. Specifically, the box plots of R and RMSE scores are shown and also compared  
431 with the results obtained through GPCC, ERA5, and GPM-ER. In terms of R, SM2RAIN-  
432 ASCAT show better performance in Italy (median R=0.67) and United States (median R=0.62),  
433 almost comparable with the other datasets; in Australia and India R-values are lower (median  
434 R=0.61 and 0.59). In the selected regions, the best product is GPCC (mainly in Australia)  
435 followed by ERA5 while GPM-ER and SM2RAIN-ASCAT performing similarly. The better  
436 performance of GPCC are expected (gauge-based dataset) and also the very good performance  
437 of ERA5 in Italy and Australia thanks to the availability of ground observations for the  
438 reanalysis. When considering the RMSE score, the results are quite different with respect to R.  
439 SM2RAIN-ASCAT is overall very good being the best (second best) product in United States  
440 (India). The ranking of the product is GPCC, SM2RAIN-ASCAT, ERA5 and GPM-ER, with  
441 the latter showing high RMSE values in United States and Australia. As obtained in previous  
442 studies ([Brocca et al., 2016](#); [Ciabatta et al., 2017](#)), the SM2RAIN approach is very good in  
443 obtaining low RMSE values thanks to its accuracy in the retrieval of accumulated rainfall.  
444 Moreover, the product accuracy is stable over time as it is not as strongly affected by the  
445 availability of satellite overpasses as in the top down approach.

446 On a global scale, the TC approach has been implemented by using the triplet SM2RAIN-  
447 ASCAT, GPM-ER and GPCC, by considering the common period 2015-2018. Theoretically,



448 the extended TC approach provides the correlation,  $R_{TC}$ , against the underlying “truth”. **Figures**  
449 **7A and 7B** show the  $R_{TC}$  maps for SM2RAIN-ASCAT and GPM-ER highlighting similar mean  
450 values (0.66 and 0.64 for SM2RAIN-ASCAT and GPM-ER, respectively). It should be  
451 underlined that the  $R_{TC}$  values are higher than those obtained in the comparison with ground  
452 observations as theoretically the metric does not contain the error in the reference ([Massari et](#)  
453 [al., 2017a](#)). The spatial pattern of the performance is quite different as demonstrated in **Figure**  
454 **7c** in which the differences between the two  $R_{TC}$  maps is shown. Again, these results underline  
455 the strong complementarity between bottom up and top down approaches (e.g., [Ciabatta et al.](#),  
456 [2017](#); [Chiaravallotti et al., 2018](#)). As expected, SM2RAIN-ASCAT performs worse over desert  
457 areas, tropical forests and complex mountainous regions. Differently, over plains and low  
458 vegetated areas SM2RAIN-ASCAT is performing better than GPM-ER, particularly in the  
459 southern hemisphere. Indeed, in Africa and South America SM2RAIN-ASCAT provides good  
460 performance (see also **Figure 7A**) thanks to the capability of the bottom up approach to estimate  
461 accumulated rainfall accurately with a limited number of satellite overpasses occurring in these  
462 areas, differently from the top down approach used in GPM-ER.

463 The box plots of  $R_{TC}$  shown in **Figure 7D** indicates that, overall, GPCC is performing  
464 similar to the two satellite products with major differences in the spatial patterns of the  
465 performance. SM2RAIN-ASCAT is performing the best among the three products in Africa,  
466 South America, central-western United States and central Asia while GPCC is performing the  
467 best in the remaining parts except the tropical region in which GPM-ER is performing very  
468 good (see **Figure 8**). If we consider only the committed area of ASCAT ([PVR 2017](#)), in which  
469 the soil moisture product is supposed to be reliable, the mean value of  $R_{TC}$  is equal to 0.72  
470 whereas in the masked area it is equal to 0.59.

## 471 **5 Data availability**

472 The SM2RAIN-ASCAT dataset is freely available at  
473 <https://doi.org/10.5281/zenodo.2591215> ([Brocca et al., 2019](#)).

## 474 **6 Conclusions**

475 In this study, we have described the development of a new SM2RAIN-ASCAT rainfall  
476 dataset highlighting the steps carried out for improving the retrieval algorithm and the pre-/post-  
477 processing of the data. The major novelties of the SM2RAIN-ASCAT rainfall dataset





478 developed here with respect to previous versions are: 1) application of SM2RAIN at full spatial  
479 resolution thus providing a gridded dataset with sampling of 12.5 km, 2) improved sampling  
480 and filtering of ASCAT soil moisture data, 3) application of monthly climatological correction.

481 The SM2RAIN-ASCAT dataset has been preliminary assessed at regional (*Figures 4 and*  
482 *6*) and global (*Figure 5, 7 and 8*) scale in terms of different performance metrics with larger  
483 emphasis on the temporal correlation, R, and the root mean square error, RMSE. The overall  
484 performances are good, mainly in terms of RMSE thanks to the capacity of SM2RAIN to  
485 accurately reproduce accumulated rainfall consistently over time. Importantly, SM2RAIN-  
486 ASCAT is found to perform even better than ground-based GPCC product over the southern  
487 hemisphere in Africa and South America, and also in central-western United States and central  
488 Asia.

489 The SM2RAIN-ASCAT rainfall dataset can now be used as input for applications such  
490 as flood prediction (similarly to [Camici et al., 2018](#) and [Massari et al., 2018](#)), landslide  
491 prediction ([Brunetti et al., 2018](#)) and novel applications for the agriculture and for the water  
492 resources management.

493

494 **Acknowledgments:** The authors gratefully acknowledge support from the EUMETSAT  
495 through the Global SM2RAIN project (contract n° EUM/CO/17/4600001981/BBo) and the  
496 “Satellite Application Facility on Support to Operational Hydrology and Water Management  
497 (H SAF)” CDOP 3 (EUM/C/85/16/DOC/15).

498 **References**

- 499 Abera, W., Formetta, G., Brocca, L., Rigon, R.: Modeling the water budget of the Upper Blue  
500 Nile basin using the JGrass-NewAge model system and satellite data. *Hydrology and*  
501 *Earth System Sciences*, 21, 3145-3165, 2017.
- 502 Brocca, L., Hasenauer, S., Lacava, T., Melone, F., Moramarco, T., Wagner, W., Dorigo, W.,  
503 Matgen, P., Martínez-Fernández, J., Llorens, P., Latron, J., Martin, C., Bittelli, M.: Soil  
504 moisture estimation through ASCAT and AMSR-E sensors: an intercomparison and  
505 validation study across Europe. *Remote Sensing of Environment*, 115, 3390-3408, 2011.
- 506 Brocca, L., Melone, F., Moramarco, T., Wagner, W.: A new method for rainfall estimation  
507 through soil moisture observations. *Geophysical Research Letters*, 40(5), 853-858,  
508 2013a.
- 509 Brocca, L., Melone, F., Moramarco, T., Wagner, W., Albergel, C.: Scaling and filtering  
510 approaches for the use of satellite soil moisture observations. In: George P. Petropoulos  
511 (ed.), *Remote Sensing of Energy Fluxes and Soil Moisture Content*, CRC Press 2013,  
512 Chapter 17, 411-426, ISBN: 978-1-4665-0578-0, 2013b.
- 513 Brocca, L., Ciabatta, L., Massari, C., Moramarco, T., Hahn, S., Hasenauer, S., Kidd, R., Dorigo,  
514 W., Wagner, W., Levizzani, V.: Soil as a natural rain gauge: estimating global rainfall  
515 from satellite soil moisture data. *Journal of Geophysical Research*, 119(9), 5128-5141,  
516 2014, 2014.
- 517 Brocca, L., Massari, C., Ciabatta, L., Moramarco, T., Penna, D., Zuecco, G., Pianezzola, L.,  
518 Borga, M., Matgen, P., Martínez-Fernández, J.: Rainfall estimation from in situ soil  
519 moisture observations at several sites in Europe: an evaluation of SM2RAIN algorithm.  
520 *Journal of Hydrology and Hydromechanics*, 63(3), 201-209, 2015.
- 521 Brocca, L., Pellarin, T., Crow, W.T., Ciabatta, L., Massari, C., Ryu, D., Su, C.-H., Rudiger, C.,  
522 Kerr, Y.: Rainfall estimation by inverting SMOS soil moisture estimates: a comparison  
523 of different methods over Australia. *Journal of Geophysical Research*, 121(20), 12062-  
524 12079, 2016.
- 525 Brocca, L., Crow, W.T., Ciabatta, L., Massari, C., de Rosnay, P., Enenkel, M., Hahn, S.,  
526 Amarnath, G., Camici, S., Tarpanelli, A., Wagner, W.: A review of the applications of  
527 ASCAT soil moisture products. *IEEE Journal of Selected Topics in Applied Earth*  
528 *Observations and Remote Sensing*, 10(5), 2285-2306, 2017.
- 529 Brocca, L.: SM2RAIN test dataset with ASCAT satellite soil moisture (Version 1.0) [Data set].  
530 Zenodo. <https://doi.org/10.5281/zenodo.2580285>, 2019.
- 531 Brocca, L., Filippucci, P., Hahn, S., Ciabatta, L., Massari, C., Camici, S., Schüller, L., Bojkov,  
532 B., Wagner, W.: SM2RAIN-ASCAT (2007-2018): global daily satellite rainfall from  
533 ASCAT soil moisture (Version 1.0) [Data set]. Zenodo.  
534 <https://doi.org/10.5281/zenodo.2591215>, 2019.
- 535 Brunetti, M.T., Melillo, M., Peruccacci, S., Ciabatta, L., Brocca, L.: How far are we from the  
536 use of satellite data in landslide forecasting? *Remote Sensing of Environment*, 210, 65-  
537 75, doi:10.1016/j.rse.2018.03.016, 2018.
- 538 Camici, S., Ciabatta, L., Massari, C., Brocca, L.: How reliable are satellite precipitation  
539 estimates for driving hydrological models: a verification study over the Mediterranean  
540 area. *Journal of Hydrology*, 563, 950-961, 2018.



- 541 Chiaravalloti, F., Brocca, L., Procopio, A., Massari, C., Gabriele, S.: Assessment of GPM and  
542 SM2RAIN-ASCAT rainfall products over complex terrain in southern Italy. *Atmospheric*  
543 *Research*, 206, 64-74, 2018.
- 544 Ciabatta, L., Brocca, L., Massari, C., Moramarco, T., Gabellani, S., Puca, S., Wagner, W.:  
545 Rainfall-runoff modelling by using SM2RAIN-derived and state-of-the-art satellite  
546 rainfall products over Italy. *International Journal of Applied Earth Observation and*  
547 *Geoinformation*, 48, 163-173, 2016.
- 548 Ciabatta, L., Marra, A.C., Panegrossi, G., Casella, D., Sandò, P., Dietrich, S., Massari, C.,  
549 Brocca, L.: Daily precipitation estimation through different microwave sensors:  
550 verification study over Italy. *Journal of Hydrology*, 545, 436-450, 2017.
- 551 Ciabatta, L., Massari, C., Brocca, L., Gruber, A., Reimer, C., Hahn, S., Paulik, C., Dorigo, W.,  
552 Kidd, R., Wagner, W.: SM2RAIN-CCI: a new global long-term rainfall data set derived  
553 from ESA CCI soil moisture. *Earth System Science Data*, 10, 267-280, 2018.
- 554 Crow, W.T., Huffman, G.F., Bindlish, R., Jackson, T.J.: Improving satellite rainfall  
555 accumulation estimates using spaceborne soil moisture retrievals. *Journal of*  
556 *Hydrometeorology*, 10, 199-212, 2009.
- 557 Crow, W.T., van den Berg, M.J., Huffman, G.J., Pellarin, T.: Correcting rainfall using satellite-  
558 based surface soil moisture retrievals: The Soil Moisture Analysis Rainfall Tool  
559 (SMART). *Water Resources Research*, 47, W08521, 2011.
- 560 Dorigo, W., Wagner, W., Albergel, C., Albrecht, F., Balsamo, G., Brocca, L., Chung, D., Ertl,  
561 M., Forkel, M., Gruber, A., Haas, D., Hamer, P., Hirschi, M., Ikonen, J., de Jeu, R., Kidd,  
562 R., Lahoz, W., Liu, Y.Y., Miralles, D., Mistelbauer, T., Nicolai-Shaw, N., Parinussa, R.,  
563 Pratola, C., Reimer, C., van der Schalie, R., Seneviratne, S.I., Smolander, T., Lecomte,  
564 P.: ESA CCI soil moisture for improved earth system understanding: state-of-the art and  
565 future directions. *Remote Sensing of Environment*, 203, 185-215, 2017.
- 566 Ebert, E.E., Janowiak, J.E., Kidd, C.: Comparison of near-real-time precipitation estimates from  
567 satellite observations and numerical models. *Bulletin of the American Meteorological*  
568 *Society*, 88(1), 47-64, 2007.
- 569 Forootan, E., Khaki, M., Schumacher, M., Wulfmeyer, V., Mehrnegar, N., van Dijk, A.I.J.M.,  
570 Brocca, L., Farzaneh, S., Akinluyi, F., Ramillien, G., Shum, C.K., Awange, J., Mostafaie,  
571 A.: Understanding the global hydrological droughts of 2003-2016 and their relationships  
572 with teleconnections. *Science of the Total Environment*, 650, 2587-2604, 2019.
- 573 Herold, N., Alexander, L.V., Donat, M.G., Contractor, S., Becker, A.: How much does it rain  
574 over land? *Geophysical Research Letters*, 43(1), 341-348, 2016.
- 575 Hou, A.Y., Kakar, R.K., Neeck, S., Azarbarzin, A.A., Kummerow, C.D., Kojima, M., Oki, R.,  
576 Nakamura, K., Iguchi, T.: The Global Precipitation Measurement (GPM) mission.  
577 *Bulletin of the American Meteorological Society*, 95(5), 701-722, 2014.
- 578 Kidd, C., Levizzani, V.: Status of satellite precipitation retrievals. *Hydrology and Earth System*  
579 *Sciences*, 15, 1109-1116, 2011.
- 580 Kidd, C., Becker, A., Huffman, G. J., Muller, C. L., Joe, P., Skofronick-Jackson, G.,  
581 Kirschbaum, D. B.: So, how much of the Earth's surface is covered by rain gauges?  
582 *Bulletin of the American Meteorological Society*, 98(1), 69-78, 2017.
- 583 Kirschbaum, D., Stanley, T.: Satellite-Based Assessment of Rainfall-Triggered Landslide  
584 Hazard for Situational Awareness. *Earth's Future*, 6(3), 505-523, 2018.



- 585 Koster, R.D., Brocca, L., Crow, W.T., Burgin, M.S., De Lannoy, G.J.M.: Precipitation  
586 Estimation Using L-Band and C-Band Soil Moisture Retrievals. *Water Resources*  
587 *Research*, 52(9), 7213-7225, 2016.
- 588 Lanza, L.G., Vuerich, E.: The WMO Field Intercomparison of Rain Intensity Gauges.  
589 *Atmospheric Research*, 94, 534-543, 2009.
- 590 Maggioni, V., Massari, C.: On the performance of satellite precipitation products in riverine  
591 flood modeling: A review. *Journal of Hydrology*, 558, 214-224, 2018.
- 592 Massari, C., Brocca, L., Moramarco, T., Trambly, Y., Didon Lescot, J.-F.: Potential of soil  
593 moisture observations in flood modelling: estimating initial conditions and correcting  
594 rainfall. *Advances in Water Resources*, 74, 44-53, 2014.
- 595 Massari, C., Crow, W., Brocca, L.: An assessment of the accuracy of global rainfall estimates  
596 without ground-based observations. *Hydrology and Earth System Sciences*, 21, 4347-  
597 4361, 2017a.
- 598 Massari, C., Su, C.-H., Brocca, L., Sang, Y.F., Ciabatta, L., Ryu, D., Wagner, W.: Near real  
599 time de-noising of satellite-based soil moisture retrievals: An intercomparison among  
600 three different techniques. *Remote Sensing of Environment*, 198, 17-29, 2017b.
- 601 Massari, C., Maggioni, V., Barbetta, S., Brocca, L., Ciabatta, L., Camici, S., Moramarco, T.,  
602 Coccia, G., Todini, E.: Complementing near-real time satellite rainfall products with  
603 satellite soil moisture-derived rainfall through a Bayesian inversion approach. *Journal of*  
604 *Hydrology*, in press, 2019.
- 605 McColl, K.A., Vogelzang, J., Konings, A.G., Entekhabi, D., Piles, M., Stoffelen, A.: Extended  
606 triple collocation: estimating errors and correlation coefficients with respect to an  
607 unknown target. *Geophys. Res. Lett.*, 41, 6229-6236, 2014.
- 608 Overeem, A., Leijnse, H., Uijlenhoet, R.: Measuring urban rainfall using microwave links from  
609 commercial cellular communication networks. *Water Resources Research*, 47(12),  
610 doi:10.1029/2010WR010350, 2011.
- 611 Pellarin, T., Louvet, S., Gruhier, C., Quantin, G., Legout, C.: A simple and effective method  
612 for correcting soil moisture and precipitation estimates using AMSR-E measurements.  
613 *Remote Sensing of Environment*, 136, 28-36, 2013.
- 614 Pendergrass, A.G., Knutti, R.: The uneven nature of daily precipitation and its change.  
615 *Geophysical Research Letters*, 45(21), 11980-11988, 2018.
- 616 “Product User Manual (PUM) Soil Moisture Data Records, Metop ASCAT Soil Moisture Time  
617 Series”: Tech. Rep. Doc. No: SAF/HSAF/CDOP3/PUM, version 0.7, 2018.
- 618 “Product Validation Report (PVR) Metop ASCAT Soil Moisture CDR products”: Tech. Rep.  
619 Doc. No: SAF/HSAF/CDOP3/PVR, version 0.6, 2017.
- 620 Rinaldo, A., Bertuzzo, E., Mari, L., Righetto, L., Blokesch, M., Gatto, M., Casagrandi, R.,  
621 Murray, M., Vesenbeckh, S.M., Rodriguez-Iturbe, I.: Reassessment of the 2010–2011  
622 Haiti cholera outbreak and rainfall-driven multiseason projections. *Proceedings of the*  
623 *National Academy of Sciences*, 109(17), 6602-6607, 2012.
- 624 Román-Cascón, C., Pellarin, T., Gibon, F., Brocca, L., Cosme, E., Crow, W., Fernández, D.,  
625 Kerr, Y., Massari, C.: Correcting satellite-based precipitation products through SMOS  
626 soil moisture data assimilation in two land-surface models of different complexity: API  
627 and SURFEX. *Remote Sensing of Environment*, 200, 295-310, 2017.



- 628 Schamm, K., Ziese, M., Raykova, K., Becker, A., Finger, P., Meyer-Christoffer, A., Schneider,  
629 U.: GPCC Full Data Daily Version 1.0 at 1.0°: Daily Land-Surface Precipitation from  
630 Rain-Gauges built on GTS-based and Historic Data.  
631 doi:10.5676/DWD\_GPCC/FD\_D\_V1\_100, 2015.
- 632 Tarpanelli, A., Massari, C., Ciabatta, L., Filippucci, P., Amarnath, G., Brocca, L.: Exploiting a  
633 constellation of satellite soil moisture sensors for accurate rainfall estimation. *Advances*  
634 *in Water Resources*, 108, 249-255, 2017.
- 635 Thaler, S., Brocca, L., Ciabatta, L., Eitzinger, J., Hahn, S., Wagner, W.: Effects of different  
636 spatial precipitation input data on crop model outputs under a Central European climate.  
637 *Atmosphere*, 9(8), 290, 2018.
- 638 Trenberth, K.E., Asrar, G.R.: Challenges and opportunities in water cycle research: WCRP  
639 contributions. *Surv. Geophys.* 35(3), 515-532, 2014.
- 640 Wagner, W., Lemoine, G., Rott, H.: A method for estimating soil moisture from ERS  
641 scatterometer and soil data. *Remote Sens. Environ.*, 70, 191-207, 1999.
- 642 Wagner, W., Hahn, S., Kidd, R., Melzer, T., Bartalis, Z., Hasenauer, S., Figa, J., de Ros-  
643 nay, P., Jann, A., Schneider, S., Komma, J., Kubu, G., Brugger, K., Aubrecht, C., Zuger, J.,  
644 Gangkofner, U., Kienberger, S., Brocca, L., Wang, Y., Bloeschl, G., Eitzinger, J.,  
645 Steinnocher, K., Zeil, P., Rubel, F.: The ASCAT soil moisture product: a review of its  
646 specifications, validation results, and emerging applications. *Meteorologische Zeitschrift*  
647 22 (1), 5-33, 2013.
- 648 Wanders, N., Pan, M., Wood, E.F.: Correction of real-time satellite precipitation with multi-  
649 sensor satellite observations of land surface variables. *Remote Sensing of Environment*,  
650 160, 206-221, 2015.
- 651 Wang, Z., Zhong, R., Lai, C., Chen, J.: Evaluation of the GPM IMERG satellite-based  
652 precipitation products and the hydrological utility. *Atmospheric research*, 196, 151-163,  
653 2017.
- 654 Zhang, Z., Wang, D., Wang, G., Qiu, J., Liao, W.: Use of SMAP soil moisture and fitting  
655 methods in improving GPM estimation in near real time. *Remote Sensing*, 11, 368, 2019.



656 **Tables**

657 **Table 1.** List of satellite, ground-based and reanalysis products used in this study (the  
 658 spatial/temporal sampling used in this study is reported).

Short name	Full name and details	Data source	Spatial/temporal sampling	Time period	References	
<b>SOIL MOISTURE</b>						
ASCAT	Advanced Scatterometer	satellite	12.5 km/daily	2007 - present	<a href="#">Wagner et al. (2013)</a>	
<b>RAINFALL</b>						
ERA5	ECMWF	reanalysis	0.25°/daily	1979 - present	<a href="https://cds.climate.copernicus.eu/cdsapp#!/dataset/reanalysis-era5-single-levels?tab=overview">https://cds.climate.copernicus.eu/cdsapp#!/dataset/reanalysis-era5-single-levels?tab=overview</a>	
GPCC	Global Precipitation Climatology Centre Full Data Reanalysis	gauge	1°/daily	1988 - present	<a href="#">Schamm et al. (2015)</a>	
IMERG Early Run	Global Precipitation Measurement Climate Prediction Center – United States	satellite	0.1°/daily	2014 - present	<a href="#">Hou et al. (2014)</a>	
CPC	Gauge-based rainfall dataset –Italy	gauge	0.5°/daily	1948 - present	<a href="https://www.esrl.noaa.gov/psd/data/gridded/data.unified.daily.conus.html">https://www.esrl.noaa.gov/psd/data/gridded/data.unified.daily.conus.html</a>	
ITA-DPC	Australian Water Availability Project – Australia	gauge	0.05°/daily	1900 - present	<a href="http://www.bom.gov.au/jsp/awap/rain/index.jsp">http://www.bom.gov.au/jsp/awap/rain/index.jsp</a>	
AWAP	India Meteorological Department - India	gauge	0.25°/daily	1901 - present	<a href="http://www.imd.gov.in/pages/services_hydromet.php">http://www.imd.gov.in/pages/services_hydromet.php</a>	
IMD	<b>SOIL TEMPERATURE and EVAPOTRANSPIRATION</b>					
ERA5	ECMWF	reanalysis	0.25°/daily	1979 - present	<a href="https://cds.climate.copernicus.eu/cdsapp#!/dataset/reanalysis-era5-single-levels?tab=overview">https://cds.climate.copernicus.eu/cdsapp#!/dataset/reanalysis-era5-single-levels?tab=overview</a>	

659



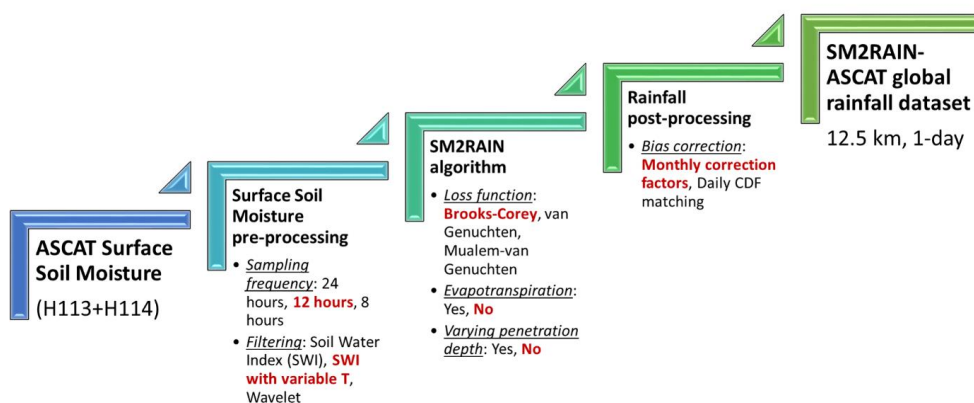
660 **Table 2.** Configurations used in the paper (SWI: Soil Water Index, BCO: Brooks-Corey, VGE:  
 661 van Genuchten, MUA: Mualem-van Genuchten, SWI-Tvar: SWI with T varying with soil  
 662 moisture, WAV: wavelet filtering, CDF: climatological correction with daily cumulative  
 663 density function matching, MON: climatological correction with monthly correction factors).

<b>Short Name</b>	<b>Filtering</b>	<b>Losses</b>	<b>Evapotranspiration</b>	<b>Depth varying</b>	<b>Climatological Correction</b>
REF	SWI	BCO	no	no	no
SWI-Tvar	SWI-Tvar	BCO	no	no	no
WAV	WAV	BCO	no	no	no
VGEN	SWI	VGE	no	no	no
MUA	MUA	VGE	no	no	no
EVAP	SWI	BCO	yes	no	no
ZVAR	SWI	BCO	no	yes	no
BC-CDF	SWI-Tvar	BCO	no	no	CDF
BC-MON	SWI-Tvar	BCO	no	no	MON

664



665 **Figures**

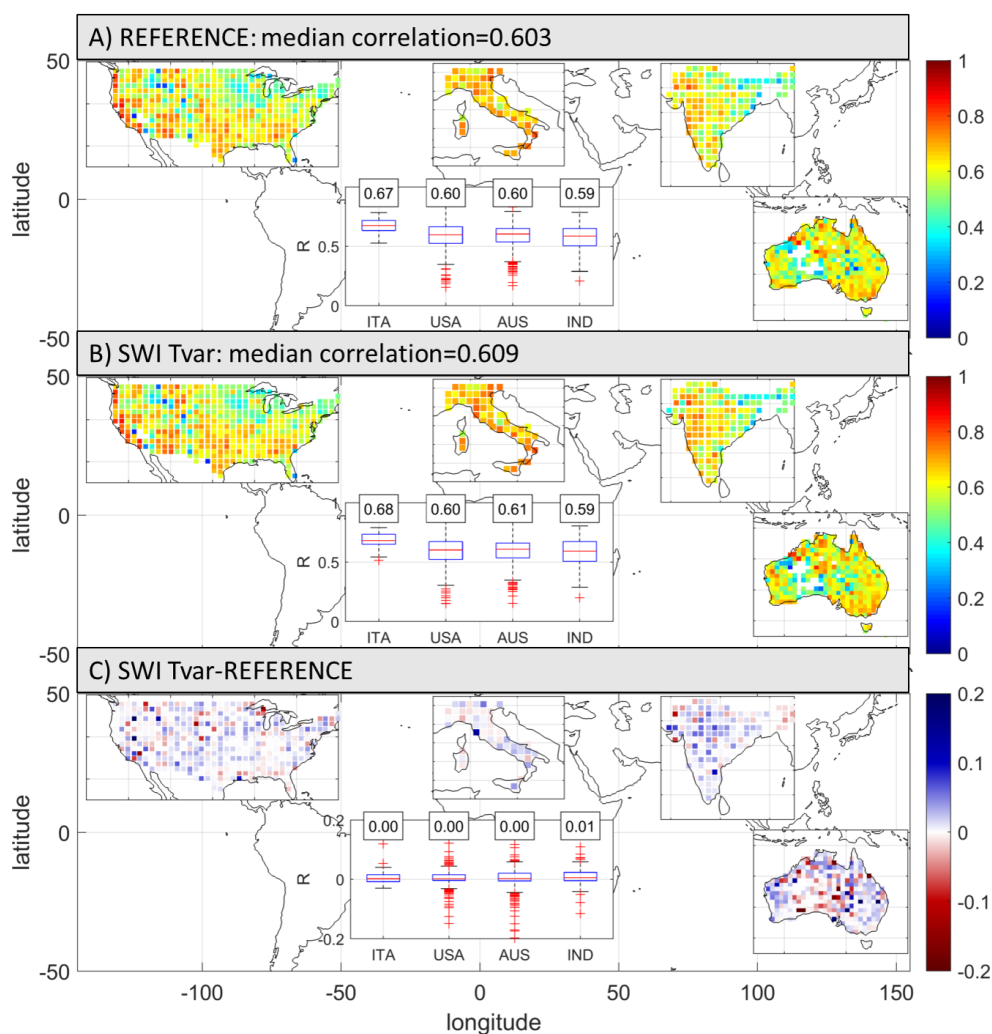


666

667 **Figure 1.** Processing steps for obtaining the SM2RAIN-ASCAT global rainfall dataset (2007-  
668 2018) from ASCAT surface soil moisture data: pre-processing, SM2RAIN algorithm, and post-  
669 processing. Each bullet represents a possible configuration that has been tested, the selected  
670 configuration is in red, bold font.

671

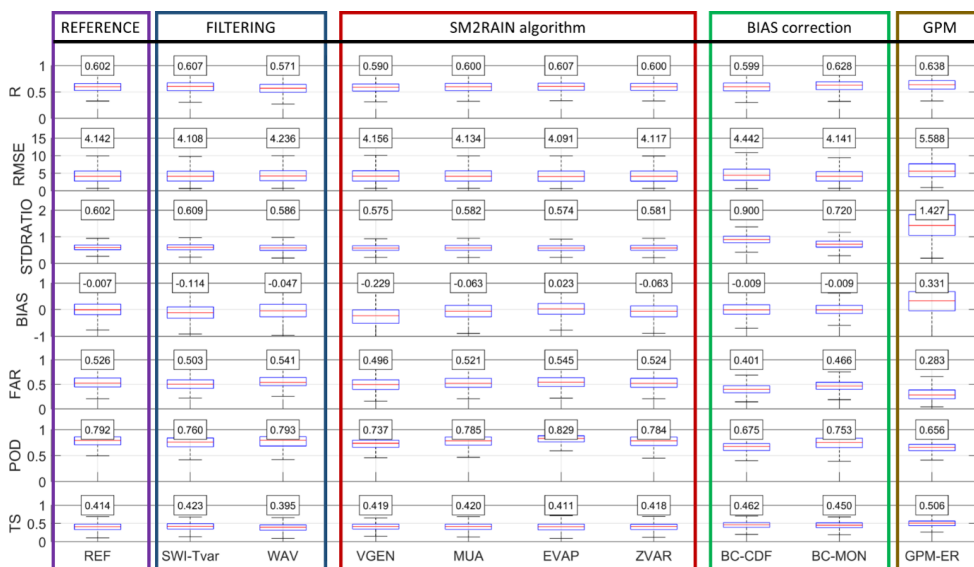




672

673 **Figure 2.** Performance of two different configurations at 1009 points in terms of Pearson's  
 674 correlation, R [-]. A) R map with reference configuration, B) R map with Soil Water Index  
 675 (SWI) filtering with variable T as a function of soil moisture, and C) R map difference (B)-(A).  
 676 The inner box plots show the R values (and R differences) split for different regions.

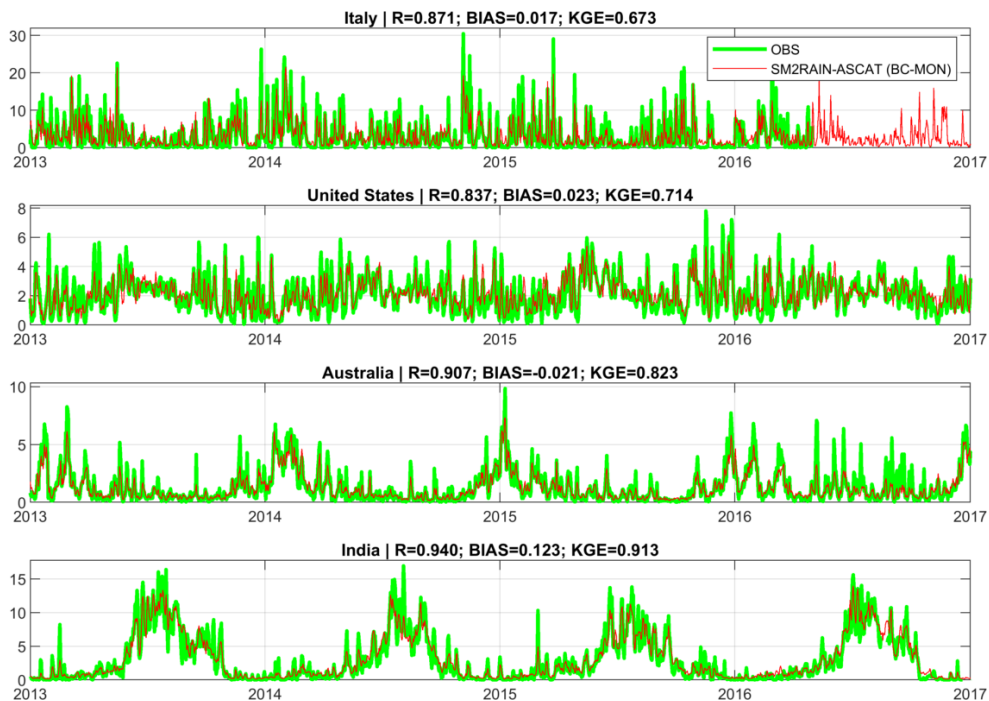
677



678

679 **Figure 3.** Performances at 1009 points in terms of Pearson’s correlation, R [-], root mean square  
 680 error, RMSE [mm/day], variability ratio, STDRATIO [-], BIAS [mm/day], false alarm ratio,  
 681 FAR [-], Probability of Detection, POD [-], and Threat Score, TS [-]. For details of the different  
 682 configurations see Table 2 (GPM-ER: GPM IMERG Early Run product).

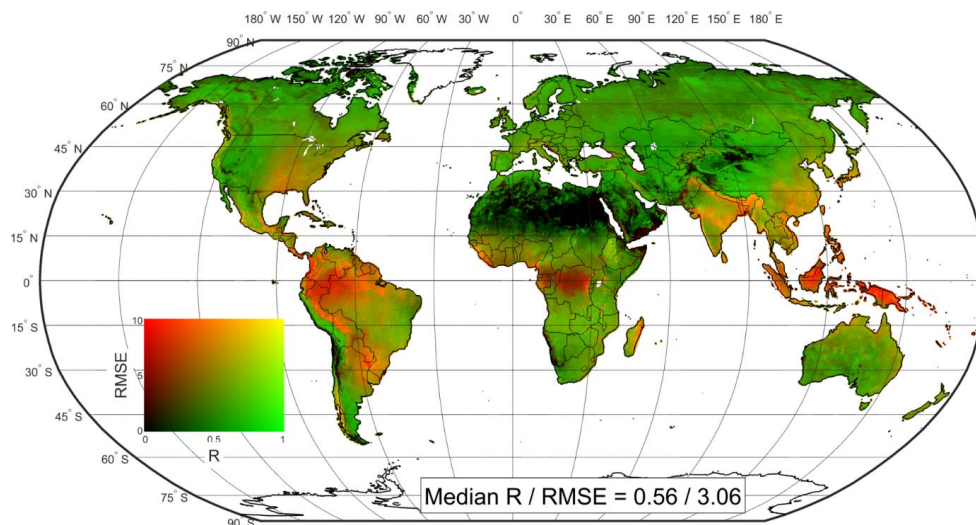
683



684

685 **Figure 4.** Time series of mean areal rainfall for the four regions for observed data, OBS, and  
686 SM2RAIN-ASCAT dataset, BC-MON configuration (R [-]: Pearson's correlation, BIAS  
687 [mm/day]: mean error, KGE [-]: Kling-Gupta efficiency).

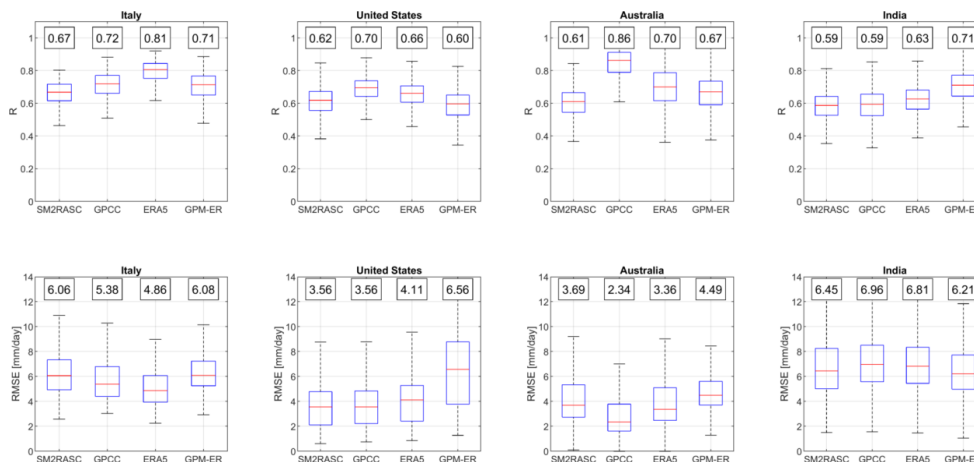
688



689

690 **Figure 5.** Pearson's correlation, R, and root mean square error, RMSE, map of SM2RAIN-  
691 ASCAT dataset compared with ERA5 reanalysis dataset used as benchmark (period 2007-  
692 2018). The analysis is carried out at 1-day and 12.5 km temporal and spatial resolution. The  
693 map shows that SM2RAIN-ASCAT dataset is performing well in the western United States,  
694 Brazil, southern and western South America, southern Africa, Sahel, southern-central Eurasia,  
695 and Australia (green colours).

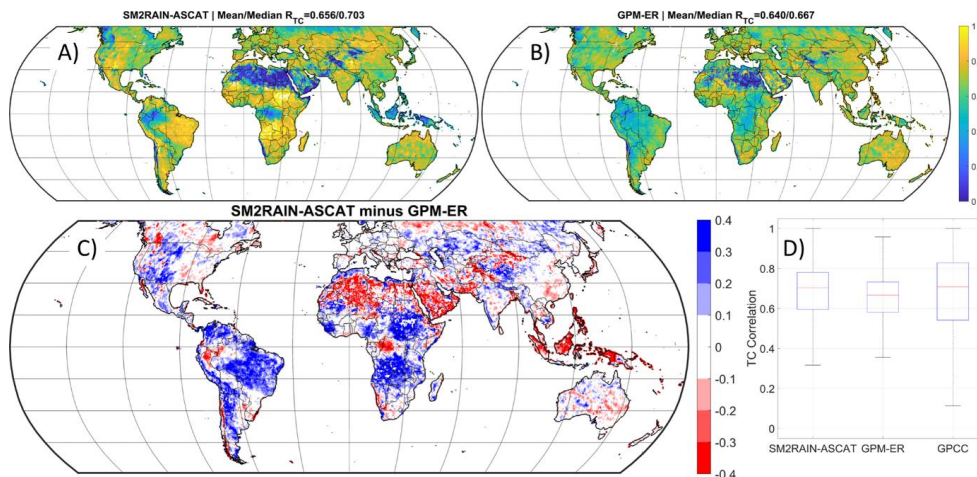
696



697

698 **Figure 6.** Regional assessment of SM2RAIN-ASCAT rainfall dataset and comparison with  
 699 GPCC, ERA5 and GPM-ER rainfall products. As reference the high-quality ground-based  
 700 datasets in Italy, United States, India and Australia are used. Top panels show the Pearson's  
 701 correlation,  $R$ , and the bottom panels the root mean square error, RMSE.

702



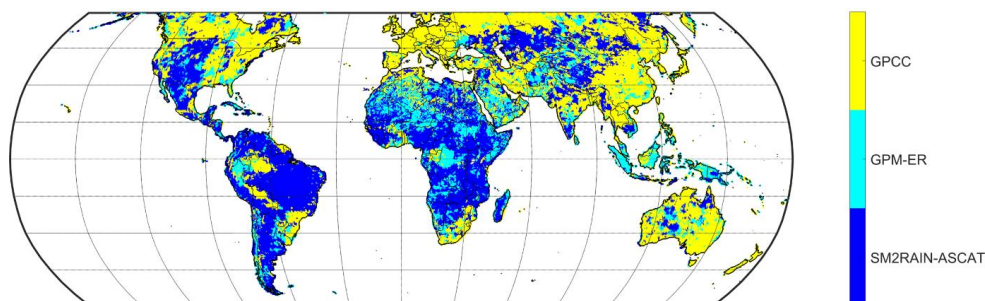
703

704 **Figure 7.** Global triple collocation, TC, results. A)  $R_{TC}$  map for SM2RAIN-ASCAT, B)  $R_{TC}$   
 705 map for GPM-ER, (C) differences between (A) and (B), i.e., blue (red) colours for pixels in  
 706 which SM2RAIN-ASCAT (GPM-ER) is performing better, and D) box plot of  $R_{TC}$  for  
 707 SM2RAIN-ASCAT, GPM-ER, and GPCC. SM2RAIN-ASCAT is performing significantly  
 708 better than GPM-ER in South America and Africa (excluding desert and tropical forest areas),  
 709 elsewhere the two satellite products perform similarly.

710



711



712

713 **Figure 8.** Best performing product based on the results of triple collocation shown in Figure 7.  
714 SM2RAIN-ASCAT is performing the best among the three products in Africa, South America,  
715 central-western United States and central Asia while GPCC is performing the best in the  
716 remaining parts of the northern hemisphere and in Australia. GPM-ER is the best product in the  
717 tropical and equatorial region.

718